

## Magnetic Flux Surface Measurements at Wendelstein 7-X

M. Otte<sup>1</sup>, T. Andreeva<sup>1</sup>, C. Biedermann<sup>1</sup>, S. Bozhnikov<sup>1</sup>, V. Bykhov<sup>1</sup>, T. Bräuer<sup>1</sup>, M. Endler<sup>1</sup>,  
J. Geiger<sup>1</sup>, G. Kocsis<sup>2</sup>, S. Lazerson<sup>3</sup>, T. Szepesi<sup>2</sup>, T. Sunn Pedersen<sup>1</sup>, and the W7-X Team

<sup>1</sup>*Max-Planck-Institute for Plasma Physics, Greifswald, Germany*

<sup>2</sup>*Wigner RCP RMI, Budapest, Hungary*

<sup>3</sup>*Princeton Plasma Physics Laboratory, Princeton, USA*

### Introduction

Magnetic confinement of stellarator-like experiments is nearly exclusively determined by the magnetic fields generated from external field coils and the vacuum magnetic field has already particle confining properties in such machines. Therefore, in contrast to a tokamak, the magnetic topology can be mapped even without plasma operation and the existence and quality of the magnetic flux surfaces can be determined well before the plasma operation.

Wendelstein 7-X (W7-X), Greifswald, Germany, has recently completed the first plasma operation phase OP 1.1 between December 2015 and March 2016. W7-X is an optimized five-periodic stellarator with a complex superconducting magnet system consisting of 50 non-planar coils of five different types which allow to create a magnetic field of up to 3.0T and a rotational transform of  $\iota_a = 1/2\pi = n/m = 5/5$ . By superimposing the field of the 20 superconducting planar field coils of two different types a variation in the edge rotational transform between  $\iota_a = 5/4$  and  $5/6$  is possible. Five normal conducting trim coils outside the cryostat vessel allow mitigation of residual magnetic error fields. Additionally, 10 normal conducting control coils installed inside the plasma vessel are foreseen for modifying the edge island structure during divertor operation starting in the second operation phase OP 1.2 [1, 2]. However, such periodic magnetic field structures are sensitive to even small magnetic error fields on the order of  $b_{nm} \sim 1 \cdot 10^{-4} B_0$ , if the toroidal and poloidal mode number  $n$  and  $m$ , are resonant with the rotational transform and can thus lead to significant distortions of flux surfaces or of the island topologies. Therefore, great care has been taken during the manufacturing of the coils and the assembly of the whole magnet system, including an optimization of the W7-X module positioning on the machine base, to minimize especially the low order  $n, m = 1, 2$  intrinsic magnetic field perturbations [3, 4].

## Diagnostic Setup

For the flux surface mapping in W7-X a dedicated diagnostic has been applied making use of a low energetic electron beam that is detected by a moveable fluorescent detector and a sensitive camera [5, 6]. The diagnostic comprises of two manipulators installed in the limiter and divertor free region in the so-called triangular plane, see Fig. 1.

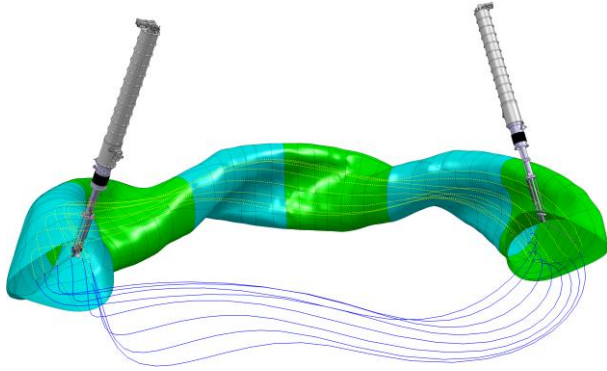


Fig. 1: Position of the two manipulators installed during OP 1.1 in the triangular plane. A single magnetic field line with its helical structure is shown in blue.

Each manipulator carries an electron gun that allows creating of an electron beam with a typical intensity of a few ten  $\mu\text{A}$  and an acceleration voltage of  $<100\text{V}$  can be generated. The rod for positioning the electron gun is coated with fluorescent material ( $\text{ZnO:Zn}$ ) and can be slowly swept through the confinement region within about 60s. Whenever crossing the field line on which the electron source is actually positioned fluorescent light in the visible spectrum is generated and a 2D Poincaré plot representing the magnetic topology of the flux surface is created. So each manipulator can either be used as source or for the detection of the electrons. This concept allows an observation of the magnetic flux surfaces at different toroidal positions without exchanging the manipulators. In addition a field line can be made visible in its whole 3D structure when operating the electron gun in background gas. Due to inelastic collisions of the electrons with a background gas such as nitrogen, argon or water vapour at a pressure of the order of  $10^{-6}$ - $10^{-4}$  mbar the trace of the electrons becomes visible.

For spatial calibration an optical reference system based on four optical fibres has been integrated in the first wall components in the proximity of the detection plane of each manipulator. The position and the orientation of the electron gun, the detection planes of the fluorescent rods and the optical fibres were determined carefully by in-vessel metrology [7]. Observation of the fluorescent light is realized utilizing sensitive CCD cameras installed in tangential ports looking onto the detection plane of the manipulators [8].

## Results from Experiments and Simulations

For the plasma operation during the initial phase OP 1.1 the plasma vessel was equipped with five poloidal limiters; one in each module. For this operation scenario a special ‘limiter’ magnetic configuration as shown in Fig. 2, right) has been tailored. The configuration was chosen such that neither large islands nor stochastic field lines exist at the last closed flux surface. Such a configuration ensures that the otherwise unprotected first wall components of the plasma vessel would have no direct contact to the plasma edge via open field lines [9].

Well before the first plasma operation the magnetic flux surface measurements have confirmed the existence and quality of the flux surfaces to the full extent [6]. For the OP1.1 ‘limiter’ configuration closed and nested flux surfaces could be determined from the magnetic axis up to the last closed flux surface. Fig. 2 shows a set of 6 individual flux surfaces generated by sweeping the fluorescent rod from close to the magnetic axis up to the 5/6 island chain. For the 5/6 island chain the field line close to the X-point is visible as well because of a higher background pressure during this measurement. As expected from simulations the experimental results showed no hints for low order  $n,m$  Fourier harmonic error fields.

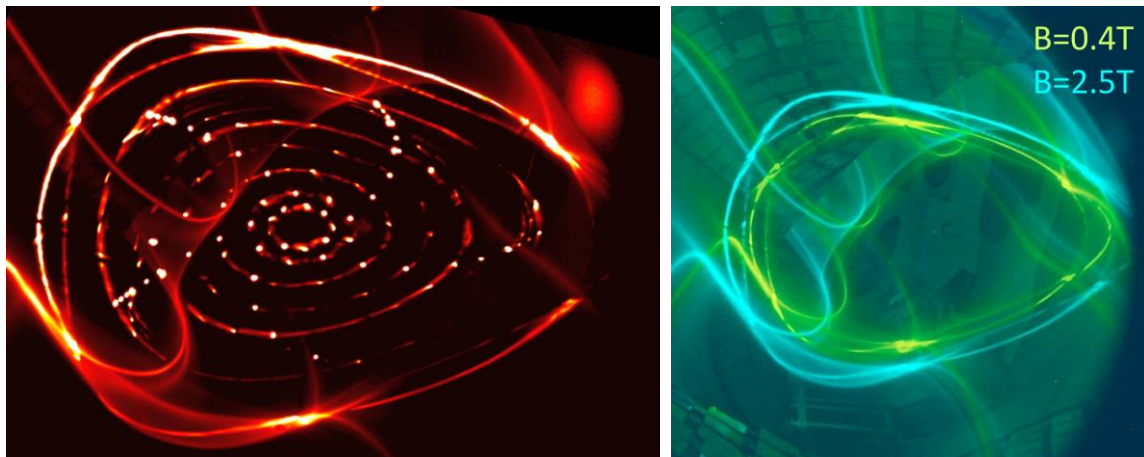


Fig. 2: Left) Six individual magnetic flux surfaces of the OP 1.1 ‘limiter’ configuration at 2.5T. At the 5/6 island the field line close to the X-point is visible as a results of the background pressure during the measurement. The bright spot on the upper right hand corner is due to reflections of in-vessel components in front of the camera port. The camera is rotated with respect to the horizontal plane. Right) Superposition of the 5/6 island chain for low (0.4T) and high magnetic field (2.5T) of the OP 1.1 ‘limiter’ configuration.

The measurements also confirm the expected elastic deformations of the non-planar field coils arising from the electromagnetic forces of the coils in the ambient magnetic field. Finite element analysis predicted an elastic deformation of about 10mm for the superconducting planar and non-planar coils. The deformation leads to a planarization of the modular field coils which is connected with a decrease in the rotational transform predicted to be about  $\sim 1.5\%$  for

2.5T in comparison to 0.4T. As a result the profile of the rotational transform is radially outward shifted including the position of the resonances. Thus the 5/6 island chain is outward shifted by a few cm for 2.5T in comparison to 0.4T but still well inside the last closed flux surface.

Furthermore, utilizing the trim coils first error field analysis for the  $b_{21}$  Fourier harmonic have been performed. For this purpose a special magnetic configuration with  $\iota = n/m = 1/2$  inside the confinement region was chosen which is resonant to an  $n = 1$  error field. By applying a sinusoidal current distribution of different amplitude and phase different magnetic islands were generated. From the extrapolated size of the island width a residual  $b_{21}$  component of  $\sim 5 \cdot 10^{-6}$  i.e. significantly below the maximum tolerable error was found [10].

In future experiments investigations at other magnetic configurations especially those which are foreseen for divertor operation and further error field studies are planned. In addition a third manipulator will be available to improve the diagnostic's capabilities.

### Acknowledgement

*This work has been carried out within the framework of the EUROfusion Consortium and has received funding from the Euratom research and training programme 2014-2018 under grant agreement No 633053. The views and opinions expressed herein do not necessarily reflect those of the European Commission.*

### References

- [1] H.S. Bosch et al., *IEEE Trans. Plasma Sci.* **42** (2014) 432
- [2] K. Risse et al., *IEEE Trans. Appl. Supercond.* **26** (2015) 4202004
- [3] H.S. Bosch et al., *Nucl. Fusion* **53** (2013) 126001
- [4] T. Andreeva et al., *Fusion Eng. Des.* **84** (2009) 408-12
- [5] T. Sunn Pedersen et al., *Nucl. Fusion* **55** (2015) 126001
- [6] M. Otte et al., *Plasma Phys. Control Fusion* **58** (2016) 064003
- [7] T. Bräuer et al., On the Geometric Accuracy of Flux Surface Diagnostic installation, submitted to *IEEE Trans. Plasma Sci.*
- [8] G. Kocsis et al., *Fusion Eng. Des.* **96-97** (2015) 808
- [9] S.A. Bozhnikov et al., *Nucl. Fusion* **56** (2016) 076002
- [10] S. Lazerson et al., First measurements of error fields on W7-X using flux surface mapping, submitted to *Nucl. Fusion*